RECOMMENDED IMPROVEMENTS TO CURRENT SHEAR-FRICTION PROVISIONS OF MODEL CODE

Pedro M. D. Santos, PhD, ISISE, Department of Civil Engineering, Polytechnic Institute of Leiria, School of Technology and Management, Portugal
Eduardo N. B. S. Júlio, PhD, ISISE, Department of Civil Engineering, University of Coimbra, Faculty of Sciences and Technology, Portugal

ABSTRACT

The shear-friction theory, first proposed by Birkeland and Birkeland (1966), was adopted by CEB-FIP Model Code 1990 to predict the longitudinal shear strength between parts of concrete members cast at different times. This is a relevant subject for different situations, such as the connection between precast members with cast-in-place parts and strengthening of existing RC members with a new concrete layer. Other situations, such as corbels; metallic supports subjected mainly to shear forces; regions near supports; and the connection between columns and foundations can also be designed using the shear-friction theory.
It is known that surface roughness plays a significant role on the bond strength of concrete-to-concrete interfaces. Recent studies, using a laser-based device specifically developed to quantify the texture of concrete surfaces, proved that roughness can be measured and, moreover, correlated with the cohesion and friction coefficients present in the Model Code's design expression. Therefore, the current qualitative assessment of the surface roughness, merely based on a visual inspection, can be replaced by an accurate and quantitative approach.
The curing conditions of the substrate concrete (old concrete) and of the added concrete layer (new concrete) are not considered either. This can have a significant influence because additional stresses can appear at the interface between both concrete layers due to differential shrinkage. Differential stiffness due to the difference between Young modulus is not addressed either. In this paper, improvements to Model Code 90's design expression for longitudinal shear strength between concretes cast at different times are recommended. Furthermore, a comparison between the design expressions proposed by the CEB-FIP Model Code 1990, the Eurocode 2 and the ACI 318 is presented.

Keywords: Repair, Rehabilitation, Standards, Specifications, Design codes.

INTRODUCTION

The "shear-friction theory" is currently adopted by all major design codes of concrete structures – CEB-FIP Model Code 1990 [1]; Eurocode 2 [2]; ACI 318 [3]; among others – to predict the shear strength between concrete layers cast at different ages. It is most adequate for the design of precast members with cast-in-place parts; strengthening of concrete bridge decks by adding an overlay; and repair and strengthening of concrete members by adding a new concrete layer.

This theory was initially proposed by Birkeland and Birkeland [4] in 1966 and the shear strength of the concrete-to-concrete interface is predicted using the following four parameters: a) the compressive strength of the weakest concrete; b) the normal stress at the interface; c) the shear reinforcement crossing the interface; and d) the roughness of the substrate surface.

The main concept of the "shear-friction theory" is that shear forces are transmitted between concrete layers by friction. The design philosophy assumes that, due to relative slippage between old and new concrete layers, the interface crack width increases, the shear reinforcement yields in tension, thus compressing the interface, and the shear forces are transmitted by friction. A "saw-tooth model" is usually adopted to exemplify this concept, Fig. 1.

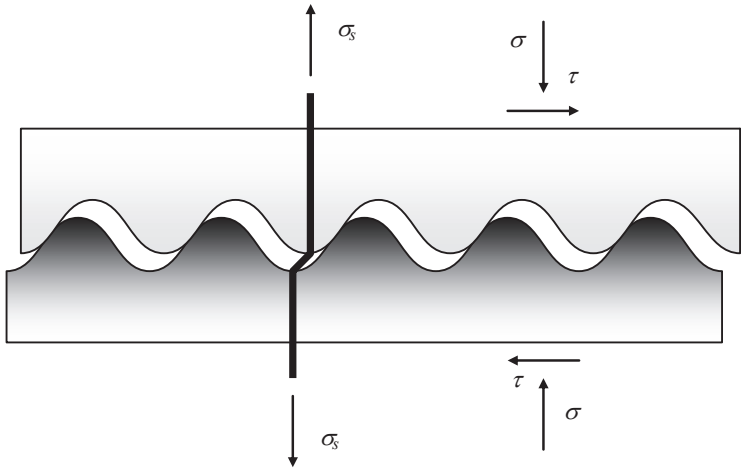

Fig. 1 Saw-tooth model.

Since composite concrete structures are the main field of application of the "shear-friction theory", parameters such as the differential shrinkage and the differential stiffness should be considered in the structural design. Nevertheless, current design codes neglect these two parameters and, therefore, the proposed design expressions can be unsafe.

This paper presents an overview about the "shear-friction theory" and the current provisions of CEB-FIP Model Code 1990 [1] on this subject, followed by a comparison between this code and the Eurocode 2 [2] and the ACI 318 [3]. The results of recent developments and new trends

on the assessment of the shear strength between concrete layers cast at different ages are presented and discussed. Finally, several improvements are proposed to the current shear-friction provisions of the CEB-FIP Model Code 1990 [1].

SHEAR-FRICTION

The design expression of the "shear friction theory", proposed by Birkeland and Birkeland [4], for the assessment of the ultimate longitudinal shear stress at the concrete-to-concrete interface is given by Eq. 1. The coefficient of friction depends on the surface preparation method and assumes the following values: a) $\mu = 1.7$, for monolithic concrete; b) $\mu = 1.4$, for artificially roughened construction joints; and c) $\mu = 0.8$ to 1.0, for ordinary construction joints and for concrete to steel interfaces.

$$v_u = \mu \rho f_y \tag{1}$$

Several researchers suggested modifications, to the design expression initially proposed by Birkeland and Birkeland [4], to increase its accuracy and to include other parameters, such as the cohesion of the interface; the weakest concrete strength; and the dowel action due to the deformation of the reinforcement bars. The most significant contributions are presented next.

In 1972, Mattock and Hawkins [5] proposed a design expression (Eq. 2), usually known as the "modified shear-friction theory", that explicitly includes the contribution of cohesion. The first term is due to cohesion of the interface, assumed constant and equal to 1.38MPa, and the second term is due to clamping stresses. The coefficient of friction is considered constant and equal to 0.8.

$$v_u = 1.38 + 0.8\left(\sigma_n + \rho f_y\right) \tag{2}$$

In 1978, Loov [6] proposed the first design expression (Eq. 3) that explicitly includes the concrete strength. The constant of the design equation was considered equal to 0.5 for initially uncracked interfaces.

$$v_u = k\sqrt{f_c\left(\sigma_n + \rho f_y\right)} \tag{3}$$

Walraven *et al.* [7], in 1987, developed an innovative "sphere model" to take into account the interaction between the aggregates, the binding paste and the interface zone and proposed a non-linear design expression (Eq. 4) calibrated using the results of a large experimental study using push-off specimens with initially cracked interfaces:

$$v_u = C_1\left(\rho f_y\right)^{C_2} \tag{4.1}$$

$$C_1 = 0.822 f_c^{\,0.406} \tag{4.2}$$

$$C_2 = 0.159 f_c^{0.303} \tag{4.3}$$

More recently, in 1997, Randl [8] proposed a design expression (Eq. 5) that explicitly includes the contribution of: *cohesion*, related to the contribution of the interlocking between aggregates; *friction*, related to the contribution due to the longitudinal relative slip between concrete layers and thus influenced by the surface roughness and the normal stress at the shear interface; and *dowel action*, related to the contribution of the flexural resistance of the shear reinforcement crossing the interface.

$$v_u = c f_c^{1/3} + \mu\left(\sigma_n + \rho k f_y\right) + \alpha\rho\sqrt{f_y f_c} \tag{5}$$

The parameters of the design expression proposed by Randl [8] are presented in Table 1. The surface roughness is quantitatively evaluated using the Sand Patch Test [9].

Table 1 Values of the design parameters proposed by Randl [8].

Surface preparation	Surface roughness R (mm)	Coefficient of cohesion c	Coefficient of friction μ		k	α	β
			($f_{ck} \geq 20$MPa)	($f_{ck} \geq 35$MPa)			
High-pressure water-blasting	≥ 3.0	0.4	0.8	1.0	0.5	0.9	0.4
Sand-blasting	≥ 0.5	0.0	0.7	0.7	0.5	1.1	0.3
Smooth	-	0.0	0.5	0.5	0.0	1.5	0.2

In all these expressions (Equations 1 to 5), v_u is the ultimate longitudinal shear stress at the concrete-to-concrete interface; μ is the coefficient of friction; ρ is the reinforcement ratio; f_y is the yield strength of the reinforcement; σ_n is the normal stress acting on the interface due to external loading; k is a constant (Loov's expression); f_c is the concrete compressive strength; c is the coefficient of cohesion; k is a coefficient of efficiency related with the reinforcement (Randl's expression); α is a coefficient for dowel action and β is a coefficient related with the concrete diagonal strut.

DESIGN CODES

According to the CEB-FIP Model Code 1990 [1], the ultimate longitudinal shear stress at the concrete-to-concrete interface (v_u) is given by the sum of the contribution of cohesion and friction. Dowel action is not explicitly considered. Depending on the finishing condition, the surface roughness can be defined as *smooth* or *rough*. A *smooth* surface can be considered if concrete is cast against steel or wooden formwork or if a trowelled or a light brushing surface

is produced ($c = 0.2$; $\mu = 0.6$). A *rough* surface can be obtained by raking, by exposing the aggregates or by providing mechanical shear keys ($c = 0.4$; $\mu = 0.9$).

$$v_u = cf_{ctd} + \mu\left(\sigma_n + \rho f_y\right) \leq 0.25 f_{cd} \tag{6}$$

Eurocode 2 [2] adopted a design expression similar to the one proposed by the CEB-FIP Model Code 1990 [1]. The main differences between both design codes are the consideration in the latter of a variable orientation of the shear reinforcement and the classification adopted for the surface roughness: *very smooth*; *smooth*; *rough*; or *indented*. The *very smooth* surface is considered as a surface cast against steel, plastic or specially prepared wooden moulds ($c = 0.025$ to 0.1; $\mu = 0.5$). The *smooth* surface is a spliformed or extruded surface or a free surface left without further treatment after vibration ($c = 0.2$; $\mu = 0.6$). The *rough* surface is a surface that has at least 3mm roughness at about 40mm spacing, achieved by raking, exposing of aggregate or other methods giving an equivalent behaviour ($c = 0.4$; $\mu = 0.7$). The *indented* surface is a surface with indentations complying with a specific geometry defined by the code ($c = 0.5$; $\mu = 0.9$).

$$v_u = cf_{ctd} + \mu\sigma_n + \rho f_y \left(\mu \sin\alpha + \cos\alpha\right) \leq 0.5 \nu f_{cd} \tag{7}$$

ACI 318 [3] proposes the simplest design expression (Eq. 8) and the ultimate longitudinal shear stress at the concrete-to-concrete interface is evaluated only considering the contribution of friction. Cohesion and dowel action are neglected.

$$v_u = \rho f_y \left(\mu \sin\alpha + \cos\alpha\right) \tag{8}$$

Four surface conditions are considered: concrete placed against hardened concrete with the surface clean but not intentionally roughened ($\mu = 0.6\lambda$); concrete placed against hardened concrete with the surface clean and intentionally roughened to a full amplitude of 6.35mm ($\mu = 1.0\lambda$); concrete placed monolithically ($\mu = 1.4\lambda$); and concrete anchored to as-rolled structural steel by headed studs or by reinforcing bars ($\mu = 0.7\lambda$). The parameter λ is a modification factor related to concrete density and shall be taken equal to: 1.00, for normal weight concrete; 0.85, for sand-lightweight concrete; and 0.75, for all lightweight concrete.

According to the ACI 318 [3], for normal weight concrete, placed monolithically or cast against hardened concrete with surface intentionally roughened, the ultimate longitudinal shear stress is upper limited by the minimum value given by $0.2f_c$, $(3.3 + 0.08f_c)$ and 11MPa. For the remaining cases, the ultimate longitudinal shear stress is upper limited by the minimum value given by $0.2f_c$ and 5.52MPa. The yield strength of the reinforcement shall not be taken greater than 414MPa.

In these expressions (Equations 6 to 8), v_u is the ultimate longitudinal shear stress at the concrete-to-concrete interface; c is the coefficient of cohesion; f_{ctd} is the tensile strength of

the weakest concrete; μ is the coefficient of friction; σ_n is the normal stress acting on the interface due to external loading; ρ is the reinforcement ratio; f_y is the yield strength of the reinforcement; f_{cd} is the design value of the concrete compressive strength; α is the angle between the shear reinforcement and the shear plane; v is a strength reduction factor; and λ is a factor related to the concrete density.

Analyzing the shear-friction provisions of these design codes it can be stated that the surface roughness has a significant influence on the bond strength of concrete-to-concrete interfaces and it is qualitatively assessed by all design codes, based in a visual inspection. Moreover, no method or device is proposed to perform a quantitative assessment of this parameter. Each design code also presents its own roughness classification, leading to different values of the coefficients of cohesion and friction for the same surface condition.

It is recognized today that the load transfer mechanism of shear forces between concrete layers cast at different ages is due to *cohesion*, *friction* and *dowel action*. The latter mechanism is neglected by all design codes, being therefore its contribution included in the other two.

Common to all design codes is the absence of any provision related with the curing conditions and, therefore, with the differential shrinkage between concrete layers. Also neglected are the added concrete and thus the differential stiffness between concrete layers.

RECENT DEVELOPMENTS

Taking into account the identified weaknesses of design codes, previously referred to, it was developed an innovative, portable and non-destructive method to perform a quantitative assessment of the surface roughness of concrete members: the *2D Laser Roughness Analyser* [10] (2D-LRA method). This new method proved to be effective, since it is possible to obtain 2D profiles of the surface texture; to compute texture parameters from these; and to correlate the latter with the bond strength of the concrete-to-concrete interface, both in shear and in tension, with high coefficients of correlation. Furthermore, the method combines all the advantages, with even higher accuracy, and overcomes all the disadvantages of existing methods [9, 11, 12].

A large experimental study [13] was also developed to assess the bond strength of the interface between concrete layers cast at different ages. Next, the materials and methods adopted in the experimental study are described, including: the curing conditions; the considered differences of ages between concrete layers; the selected bond tests; the adopted concrete mixture; the instrumentation used to measure the concrete shrinkage; and the techniques adopted to prepare the interface surface and increase its roughness.

MATERIALS AND METHODS

Two different curing conditions were considered: a) curing inside the laboratory, under normal conditions of work; and b) curing in the exterior of the laboratory, with the specimens directly exposed to the environmental conditions such as solar radiation, rain and wind. The temperature and the relative humidity were recorded using a hygro-thermograph for both conditions. The average (AVG), the standard deviation (STD) and the coefficient of variation (COV) of both parameters are presented in Table 2.

Table 2 Temperature and relative humidity.

Curing condition	Period	Temperature			Relative Humidity		
		AVG (ºC)	STD (ºC)	COV (%)	AVG (%)	STD (%)	COV (%)
Laboratory	Oct/06 - Feb/07	18.2	2.9	15.9	70.3	12.6	17.9
Exterior	Feb/07 - May/07	17.5	5.2	29.4	70.8	22.3	31.5

To study the influence of the differential shrinkage between concrete layers, three different situations for the time gap between casting the substrate and the added concrete layer were considered: 28 days; 56 days; and 84 days.

Combining the curing conditions with the differences of ages, six sets of specimens were produced: L28, L56 and L84 (L series); and E28, E56 and E84 (E series), where L reports to the specimens cured in the laboratory and E to those cured in the exterior, followed by the difference of ages between concrete layers.

To assess the bond strength of the concrete-to-concrete interface, respectively in shear and in tension, the slant shear test [14] and the splitting test [15] were selected. The adopted geometry for the slant shear specimens was a 150×150×450mm^3 prism with the shear plane at 30º to the vertical. The adopted geometry for the splitting specimens was a 150mm cube with the interface at middle height. For quality control purposes cubic specimens [16] were adopted.

The adopted concrete mixture was designed considering Portland cement type I 52.5R (350kg) and four different aggregates: fine sand (295kg); coarse sand (640kg); fine limestone crushed aggregates (375kg); and coarse limestone crushed aggregates (545kg). A commercial admixture (3.675kg) was used to increase the initial strength of hardened concrete by reducing the water (150kg) need, although keeping the workability of fresh concrete.

Twelve concrete mixtures were necessary to cast all sets of specimens. Since the major goal of the research study was to investigate the influence of the differential shrinkage on the bond strength of concrete-to-concrete interfaces, a single concrete composition was adopted. Nevertheless, the differential stiffness between concrete parts was also considered in the analysis of results since small differences were observed in the compressive strength of the cubic specimens used for control purposes, Table 3.

The concrete shrinkage was recorded for both curing conditions, using in each case two prismatic 150×150×600mm^3 specimens [17]. Deformations were measured using, in each specimen, two Mitutoyo 2118SB-10 transducers attached to two calibrated steel bars positioned at a distance of 300mm, Fig. 2. An average value, computed from two concrete specimens, was considered.

Table 3 – Compressive strength and age of concrete at test date.

Series	Concrete Layer	Compressive Strength * (*MPa*)	Age at Test (days)
L28	Substrate	79.3	56
	Added	66.4	28
L56	Substrate	86.0	84
	Added	80.5	28
L84	Substrate	86.4	112
	Added	72.6	28
E28	Substrate	78.9	56
	Added	68.3	28
E56	Substrate	77.6	84
	Added	71.1	28
E84	Substrate	81.9	112
	Added	69.9	28

* Average value, obtained from three concrete specimens according to EN 12390-3 [16] on the day of the test.

The evolution with time of concrete shrinkage is presented in Fig. 3. The experimental shrinkage strain was compared with the theoretical value evaluated according to the Eurocode 2 [2]. The average compressive strength was 67.3MPa and 75.8MPa for specimens cured in the laboratory and in the exterior, respectively. The average relative humidity was 70.3% and 70.8% measured in the laboratory and in the exterior, respectively.

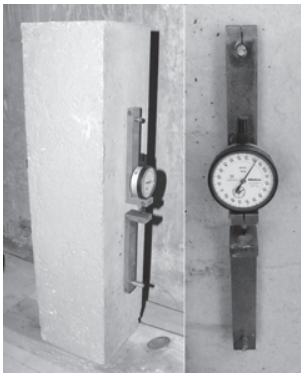

Fig. 2 Shrinkage measurement.

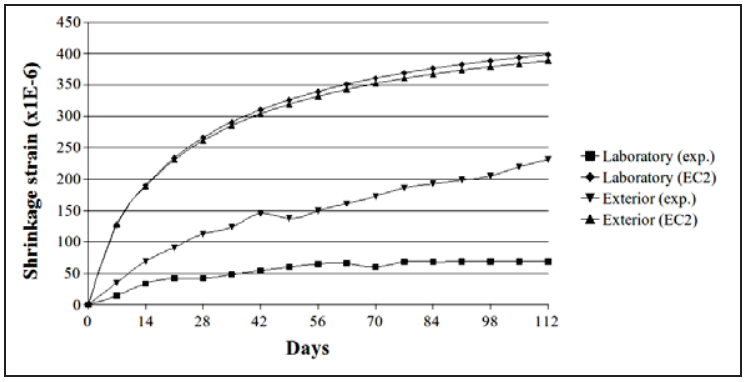

Fig. 3 Evolution of concrete shrinkage strain.

The shrinkage prediction according to the Eurocode 2 [2] proved to be very conservative. The resemblance between the theoretical predictions, for both curing conditions, is justified taking into account that the average relative humidity is also approximately equal in both situations. The difference between the experimental measurements, for both curing conditions, is explained with the different daily fluctuations of the relative humidity, Table 2. Moreover, the specimens stored outside the laboratory were directly exposed to rain and wind, with respectively a negative and a positive effect in shrinkage increase.

The interface surface between the substrate and the added concrete layer was prepared using different methods, Fig. 4. Left as-cast (LAC) against steel formwork was considered the reference situation. The roughness of the hardened concrete was increased by: a) wire-brushing (WB); b) sand-blasting (SAB); and c) shot-blasting (SHB). Hand-scrubbing (HS), a technique commonly used to prepare fresh concrete members in the precast industry, also known as "raking", was also considered.

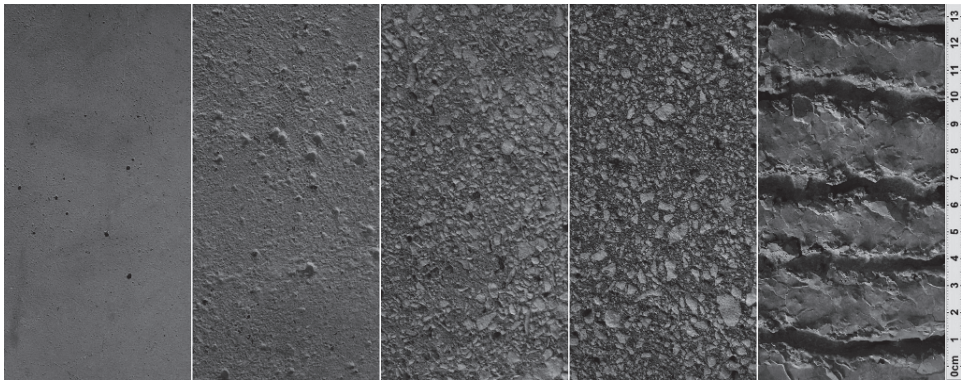

Fig. 4 Surface preparation (pictures at scale).

The surface roughness was quantified adopting the 2D-LRA method [9]. The roughness parameter *Maximum Valley Depth* (R_v) was selected to be correlated with the bond strength of the interface, both in shear and in tension. Ten texture profiles, with an evaluation length of 150mm, were measured for each surface condition and the adopted roughness parameter directly computed from the primary profile, i.e., without filtering. The *Maximum Valley Depth* (R_v), taken as the average of the values computed from each of the ten profiles, assumed the following values: 0.119mm, for the left as-cast surface; 0.473mm, for wire-brushing; 0.604mm, for sand-blasting; 0.899mm, for shot-blasting; and 2.350mm, for hand-scrubbing.

TASKS DESCRIPTION

For each considered situation – curing condition; surface preparation; and difference of age between the substrate and the added concrete – five slant shear specimens and five splitting specimens were cast.

The hand scrubbed surfaces were prepared while the concrete was still fresh, approximately two hours after casting the substrate. All the remaining surface treatments, wire-brushing; sand-blasting and shot-blasting, were later executed with hardened concrete.

The slant shear specimens and the splitting specimens were cast using two different methods since the hand-scrubbed treatment had to be applied on fresh concrete surfaces. All hand-scrubbed specimens were cast with the interface placed horizontally, while the remaining specimens were cast with the interface placed vertically. The concrete was placed vertically, being the specimens cast side by side, Fig. 5a) (top view). For the hand-scrubbed specimens, the substrate concrete was cast with the formwork at 30º to the horizontal and having only one specimen at the bottom. This way, the interface surface was horizontal and could be treated while fresh, Fig. 5b) (side view). Each hardened specimen was later placed again inside the formwork and the added concrete was cast, Fig. 5c) (top view). A hardened concrete cube of 150mm, protected with a plastic sheet, was placed inside the steel formwork to adjust the height.

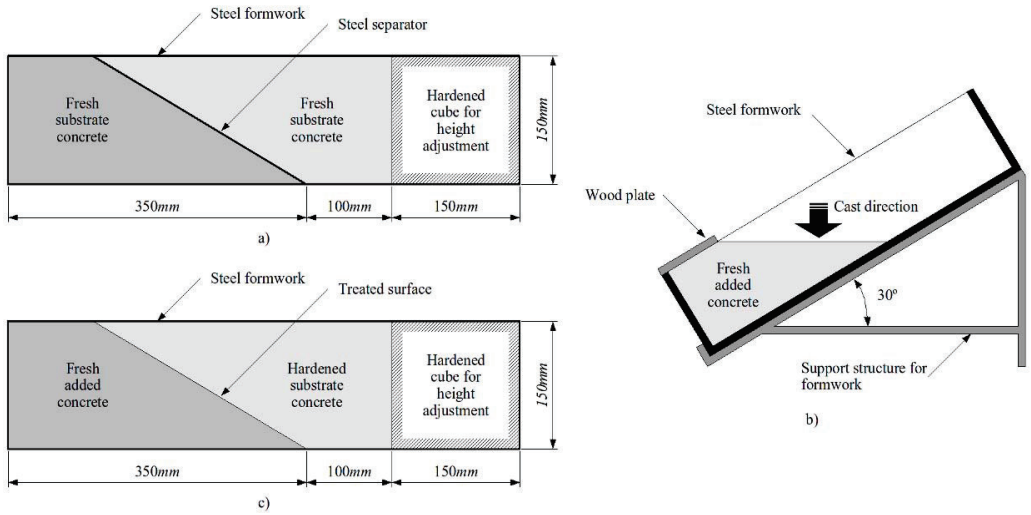

Fig. 5 Concrete placement for the slant shear test.

For the splitting specimens and for all surface treatments, with the exception of the hand-scrubbed, a hardened concrete half cube of 150mm, protected with a plastic sheet, was placed vertically inside the steel formwork. The substrate concrete was then cast in the remaining space, Fig. 6a) (side view). After demolding, the surface of each half splitting specimen was subjected to a roughness treatment. For the specimens treated with the hand-scrubbed method, the half hardened cube was placed horizontally at the bottom of the formwork allowing the surface of the added half to be treated while the concrete was still fresh, Fig. 6b) (side view). The added concrete was cast afterwards, adopting the same procedure previously described, Fig. 6c) (side view).

After surface preparation, specimens were cleaned with compressed air to remove dust and stored again under the specified curing conditions. Before placing back the specimens inside the formwork to cast the added concrete, these were cleaned with compressed air once more.

All specimens were dry when the added concrete was placed. After 28, 56 and 84 days, and for each curing condition, the added concrete was cast on the substrate concrete. Two days later, the composite specimens were removed from the formwork and placed again under the considered curing conditions.

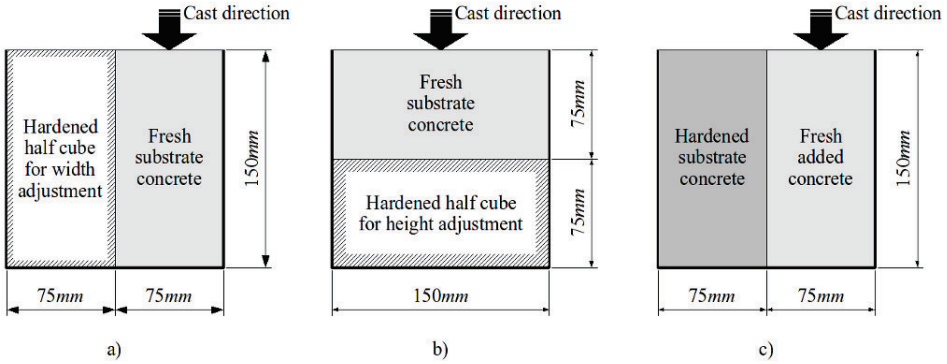

Fig. 6 Concrete placement for the splitting test.

When the added concrete reached 28 days of age, the specimens were tested in compression using a standard testing machine. The adopted load rate was 1kN/s for the splitting specimens; 5kN/s for the slant shear specimens; and 10kN/s for the cubic specimens for compressive strength control.

EXPERIMENTAL RESULTS

Two distinctive failure modes were observed: adhesive failure (interface debonding) and cohesive (monolithic) failure. All splitting specimens presented adhesive failures while the slant shear specimens presented both adhesive and cohesive failures, Fig. 7.

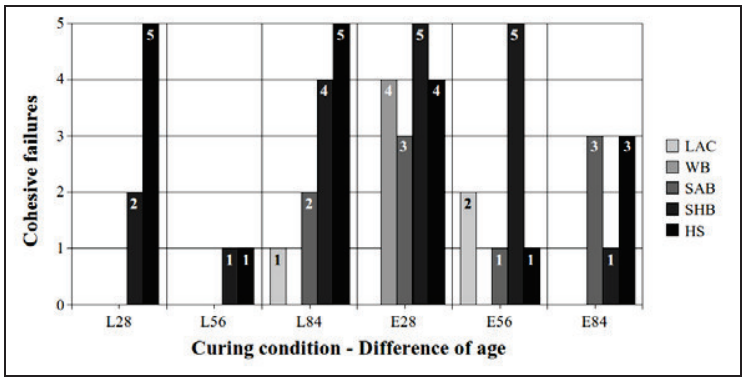

Fig. 7 Number of monolithic failures in shear.

The results obtained with the tested concrete specimens can not be directly compared since, besides the differences between failure modes, differences between concrete strengths were also measured. For all the reasons presented, the Mohr-Coulomb criterion was adopted to determine the pure shear strength for all slant shear specimens and the results analysis was

performed based on this parameter. The failure envelope of both substrate concrete and added concrete was defined using the experimental value of the compressive strength and the analytical tensile strength, predicted according to the Eurocode 2[2]. The failure envelope of the interface was defined using the experimental values of the bond strength in shear and in tension, assessed using the slant shear test and the splitting test, respectively. In Fig. 8, it is presented the bond strength in shear, given by the pure shear strength. In Fig. 9 the bond strength in tension is presented.

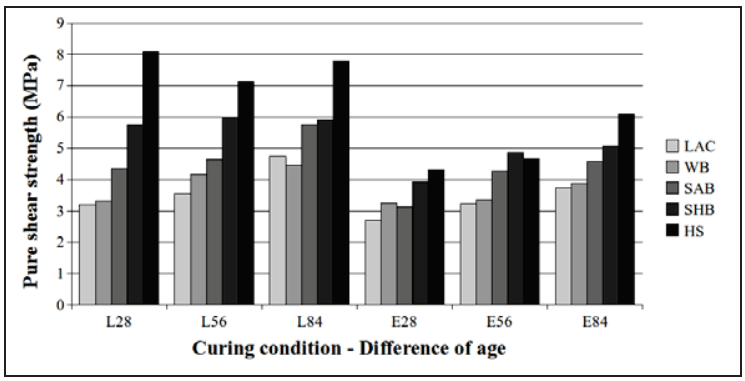

Fig. 8 Bond strength in shear.

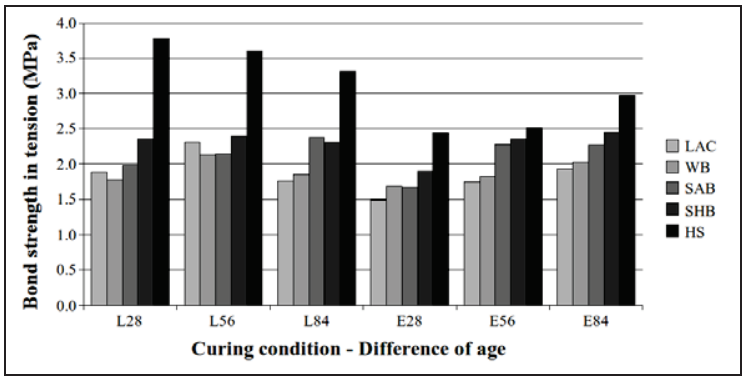

Fig. 9 Bond strength in tension.

From Fig. 8 it can be concluded that the pure shear strength of the interface increases, for both curing conditions, with the increase of the surface roughness. Three exceptions were identified: the wire-brushed surface for the L84 series; the sand-blasted surface for the E28 series; and the hand-scrubbed surface for the E56 series.

It can also be observed that the pure shear strength increases, for both curing conditions, with the increase of the difference of ages between the substrate concrete and the added concrete layer. Three exceptions were also identified for the L series, one for the shot-blasted surface and two for the hand-scrubbed surface. This result was not expected since the bond strength of the interface is supposed to decrease with the increase of differential shrinkage which increases with the difference of ages between concrete layers.

The assessment of the bond strength in tension, with the splitting test, proved to be inconclusive. The evolution of the bond strength, with the increase of the surface roughness and with the increase of the difference of ages between concrete layers, is not clear. Therefore, when comparing the results obtained with this bond test, with the results achieved with the slant shear test, it appears that this test is unsuitable for this purpose, i.e. less sensitive to these parameters.

The curing conditions also revealed a significant influence. The specimens stored in the exterior led, as expected, to lower values of the pure shear strength, with an average decrease of 1.12MPa, to which corresponds a decrease of 19%.

The concrete specimens were cast in six series using the same concrete mixture. Nevertheless, different values were obtained for the compressive strength at the test date. Although small, these differences have influence on the Young modulus of each concrete layer and, consequently, on the differential stiffness of the composite concrete element. According to several researchers [18, 19], the increase of the differential stiffness between concrete layers changes the stress distribution at the interface and stress concentrations are observed at both ends. The slant shear specimens corroborated these conclusions and broken corners were observed precisely at both ends of the interface.

Despite the reduced number of concrete specimens, it was observed an increase of the number of cohesive failures with the increase of the difference between the Young modulus of both concrete layers, evaluated using the Eurocode 2 [2] from the compressive strength presented in Table 3, which corroborates the results of previous studies [18]. The existence of a correlation between these two parameters, cohesive failure and differential stiffness, is extremely important since it means that it is possible to change the failure mode of a composite concrete element by designing the differential stiffness between both concrete layers.

For the slant shear specimens, the number of cohesive failures, Fig. 7, increased with the increase of the surface roughness of the interface, presenting 3, 4, 9, 18 and 19 failures for the left as-cast, wire-brushed, sand-blasted, shot-blasted and hand-scrubbed surfaces, respectively.

NUMERICAL MODELING

In order to understand the unexpected increase of the bond strength with the increase of the differential shrinkage, a numerical study was conducted using commercial finite elements software (LUSAS [20]).

A 3D model of the slant shear specimen was built using a finite elements mesh with twenty nodes hexahedrons, Fig. 10. Linear material behavior was assumed. The adopted geometry was a prism with a square cross section of 150mm width and a height of 450mm with the shear plane at 30º with the vertical. Only the nodal displacements at the top and bottom faces were restrained.

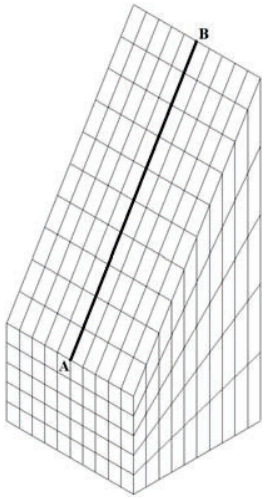

Fig. 10 Finite elements mesh.

The material and time-dependent properties of concretes used in the experimental study were adopted in the 3D model to perform the analysis of the combined effect of differential shrinkage and differential stiffness with the compressive loading at the test date.

For the shrinkage strain of the substrate concrete cured under laboratory conditions, the following values were adopted: 65.0×10^{-6}, 68.3×10^{-6} and 69.2×10^{-6} for a difference of age between both concrete layers of 28, 56 and 84 days, respectively. For the shrinkage strain of the substrate concrete cured in the exterior, the corresponding following values were adopted: 149.2×10^{-6}, 192.5×10^{-6} and 230.8×10^{-6}, respectively. The shrinkage strain of the added concrete was considered equal to 47.1×10^{-6} and 112.5×10^{-6}, at the age of 28 days, for curing under laboratory conditions and curing in the exterior, respectively.

The Young modulus of the substrate concrete and of the added concrete was assumed according to the Eurocode 2 [2], using the values obtained for the compressive concrete strength at the test date. The coefficient of Poisson was considered equal to 0.2.

The vertical displacement imposed to simulate the compression of the testing machine was taken equal to 40% of the average compressive strength of a C50/60 strength class. This value was adopted since it is used, as suggested by Eurocode 2 [2], for the determination of the secant modulus of elasticity of concrete.

The distribution of shear, normal and equivalent stresses (von Mises stress), along the mean line of the interface (segment AB in Fig. 10), is presented in Fig. 11 to 13, respectively.

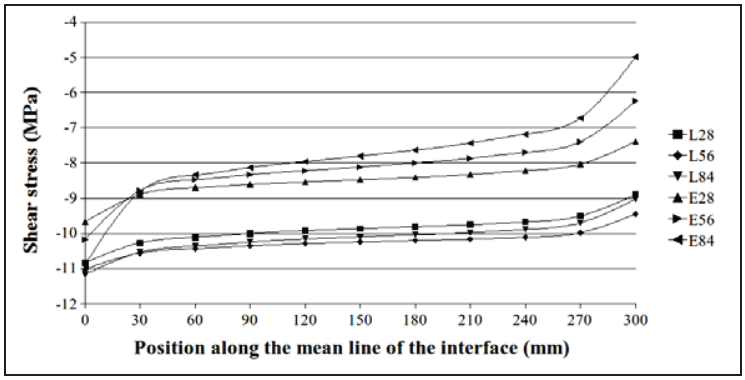

Fig. 11 Shear stress distribution.

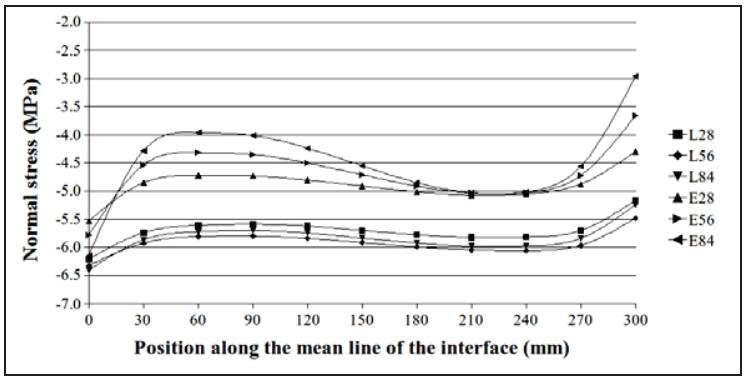

Fig. 12 Normal stress distribution.

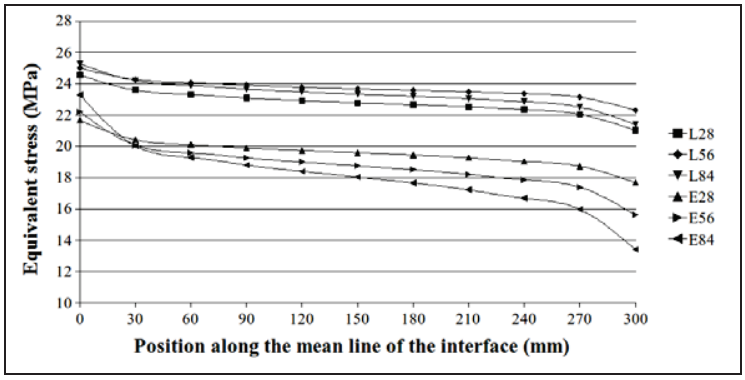

Fig. 13 Equivalent stress distribution.

As expected, stresses at the interface increased with the increase of the differential shrinkage. At the test date, the concrete specimens are already subjected to a stress state due to differential shrinkage. Therefore, with compressive loading, the tension stresses due to differential shrinkage disappear from the interface. The combined effect of the differential shrinkage, differential stiffness and compressive loading during testing revealed that the failure load increases with the difference of ages between concrete layers and, thus, with the differential shrinkage, opposing to what was first expected. This can be observed in Fig. 11 to 13, respectively for shear, normal and equivalent stresses at the interface, with the only

exception of L28 series. It should be added that comparisons between L and E series, for the same difference of ages, cannot be made since other influencing parameters, besides shrinkage, are also present but were not assessed.

The numerical model also corroborated the experimental observations related with the differential stiffness. With the increase of the differential stiffness, stress concentrations occur at both ends and the stress distribution assumes an S-shaped form. Analyzing the evolution of the normal stress with the shear stress, it is possible to conclude that for the same level of the latter, the corresponding normal stress increases with the increase of the differential stiffness between concrete parts, Fig. 14. This type of evolution can explain the different failure modes observed for the slant shear specimens.

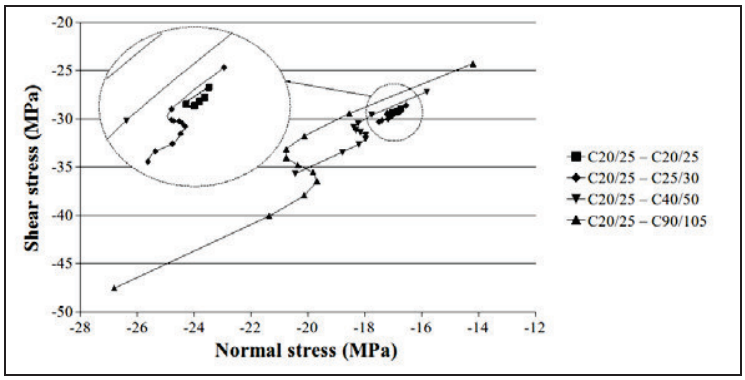

Fig. 14 Comparison of normal stress versus shear stress in the interface.

CONCLUSIONS AND RECOMMENDATIONS

From the analysis of codes and published research it can be concluded that the roughness of the concrete substrate has a very significant influence on the bond strength of concrete-to-concrete interfaces. Moreover, it can be stated that in all design codes this parameter is qualitatively assessed, although each one presents its own classification. Furthermore, it can be seen that, even though it is recognized today that the load transfer mechanism at the concrete-to-concrete interface is due to cohesion, friction and dowel action, the latter is neglected in all design codes.

Common to all design codes is the absence of any provision related with the curing conditions and, therefore, with the differential shrinkage between concrete parts. Also neglected is the added concrete and thus the differential stiffness between concrete parts.

Taking into account the weaknesses of the design codes referred to, it is proposed that a quantitative methodology be adopted to avoid the subjective assessment of the surface roughness. For that purpose, the authors developed a measuring device, named *2D Laser Roughness Analyser*, and proposed an innovative and non-destructive method to predict the bond strength of concrete-to-concrete interfaces. The method proved to be effective, presenting the advantages of existing methods and overcoming all their disadvantages.

The curing conditions adopted in the experimental study showed to have a significant influence on the bond strength of the concrete-to-concrete interface. The average values of the temperature and relative humidity were very similar for both conditions but the coefficient of variation, for the curing in the exterior of the laboratory, was approximately the double relatively to the curing inside the laboratory, due to higher daily fluctuations of both parameters. Comparing both curing conditions, a significant decrease of the bond strength was observed from the curing in laboratory to the curing in exterior conditions. The average decrease of the bond strength was of 19%.

The prediction of shrinkage by the Eurocode 2[2] showed to be very conservative. The experimental measurements, for both curing conditions, were considerably different and are mainly due to daily fluctuations of the relative humidity and temperature and also to the direct exposure of the concrete specimens to rain and wind outside the laboratory.

As expected, the bond strength of the concrete-to-concrete interface increased with the increase of the surface roughness. The surface preparation proved to have a significant influence on the achieved bond strength, as demonstrated by comparing the bond strength of the left as-cast surface with the remaining four surface conditions. It can be obtained an increase of the bond strength higher than 100% only by making an adequate surface preparation.

The developed numerical model corroborated the experimental observations, namely the unexpected increase of the bond strength with the increase of the difference of ages between concrete layers and the stress concentration at both ends of the slant shear specimen. It also demonstrated that the failure mode can be modified by designing the differential stiffness between concrete layers.

The numerical model also showed that the compressive loading eliminates the tension stresses at the interface of slant shear specimens, due to the differential shrinkage. Therefore, with the increase of the difference of ages between concrete layers, corresponding to a higher differential shrinkage, the failure load of the slant shear specimens also increases. This beneficial effect should be verified for other structural concrete-to-concrete interfaces, thus to other stress states.

The research study proved that both differential shrinkage and differential stiffness can have a significant influence on the behavior of concrete-to-concrete interfaces, namely on the bond strength and, as a consequence, on the failure mode. Therefore, it can be stated that the design expressions of current design codes should be improved to incorporate the consideration of these parameters, thus increasing their accuracy.

Based in this study, the authors suggest that the coefficients of cohesion and friction, present in the shear-friction design expressions, should be predicted by the means of a texture parameter. The following expressions are proposed:

$$c_d = \frac{1.062 R_{vm}^{\ 0.145}}{\gamma_{coh}} \tag{9}$$

$$\mu_d = \frac{1.366 R_{vm}^{\ 0.041}}{\gamma_{fr}} \tag{10}$$

where:

c_d is the design coefficient of cohesion;
μ_d is the design coefficient of friction;
R_{vm} is the Mean Valley Depth of the primary profile of the surface in millimetre;
γ_{coh} is the partial safety factor for the coefficient of cohesion;
γ_{fr} is the partial safety factor for the coefficient of friction.

The proposed expressions were obtained by adjusting a power function to the experimental values of the coefficients of cohesion and friction, Fig. 15, determined for five different surface conditions: left as-cast (LAC); wire-brushing (WB); sand-blasting (SAB); shot-blasting (SHB) and hand-scrubbing (HS) or raking. Based in the coefficient of variation of both coefficients, the authors propose the values of 2.6 and 1.2 for the partial safety factors of the coefficients of cohesion and friction, respectively.

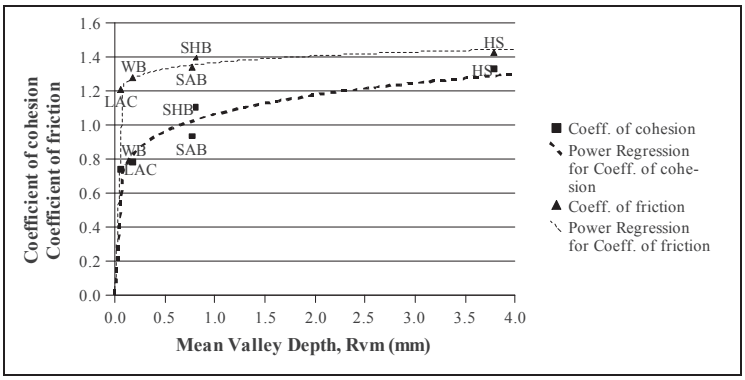

Fig. 15 Correlation between the Mean Valley Depth (R_{vm}) and the coefficients of cohesion and friction.

For uniform interface surfaces, the roughness must be measured with a minimum accuracy of 10 micrometer; then, the Mean Valley Depth (R_{vm}) has to be determined, taken as the average value obtained considering at least ten 2D primary profiles.

Uniform interface surfaces can be considered as those resulting from: as-cast against steel, plastic or specially prepared wooden moulds; slipformed or extruded surface; free surface left without further treatment after vibration; or surfaces prepared by wire-brushing, sand-blasting, shot-blasting, water-blasting or other equivalent methods.

When no reinforcement crossing the interface is provided, the ultimate longitudinal shear stress at the concrete-to-concrete interface (v_u) is given by:

$$v_u = c_d f_{ctd} \leq 0.25 f_{cd} \tag{11}$$

When reinforcement crossing the interface is provided, the ultimate longitudinal shear stress is given by:

$$v_u = \mu_d \left(\sigma_n + \rho f_y \right) \leq 0.25 f_{cd} \tag{12}$$

The proposed methodology is adequate for uniform interface surfaces. For other cases, such as non-uniform interface surfaces obtained by raking or presenting indentations, the values of the coefficients of cohesion and friction should be evaluated for each specific case, i.e., for each interface geometry.

Finally, since recent investigations [13] proved that differential shrinkage and differential stiffness can have a significant influence on the shear strength of the interface between concretes cast at different times, these effects should at least be mentioned in codes.

The differential shrinkage between both concrete parts should be taken into consideration in the design and evaluated on site for each specific case. The influence of temperature should also be considered in design.

The differential stiffness between both concrete parts should be taken into consideration in the design. The Young modulus of the added concrete layer should never be taken smaller than that of the substrate concrete.

Additionally, other requirements should be satisfied. In cases where the joint can be significantly cracked, the coefficient of cohesion should be taken as zero, for all types of interface surfaces. Under fatigue or dynamic loads, the design shear resistance at the interface due to cohesion should not be considered.

ACKNOWLEDGMENTS

The authors acknowledge the financial support of the Portuguese Science and Technology Foundation (FCT), PhD Grant number SFRH/BD/25510/2005. Acknowledgements are extended to the companies Maprel – Empresa de Pavimentos e Materiais Pré-Esforçados Lda, Sika Portugal SA, AFAssociados – Projectos de Engenharia SA, Weber Cimenfix, Cimpor – Cimentos de Portugal, Betão-Liz and Euro-Planning – Engenharia & Gestão Lda also for their financial support.

REFERENCES

1. CEB-FIP Model Code, Comité Euro-International du Béton, Secretariat Permanent, Case Postale 88, CH-1015 Lausanne, Switzerland, 1990, 437 p.
2. Eurocode 2, "Design of concrete structures - Part 1-1: General rules and rules for buildings", European Committee for Standardization, Avenue Marnix 17, B-1000 Brussels, Belgium, 2004, 225 p. (with corrigendum dated of 16 January 2008)
3. ACI 318, "Building code requirements for structural concrete (ACI 318-08) and commentary", American Concrete Institute, PO Box 9094, Farmington Hills, MI 48333-9094, USA, 2008, 471 p.
4. Birkeland, P.W. and Birkeland, H.W., "Connections in precast concrete construction", *ACI Journal*, V. 63, No. 3, March 1966, pp. 345-368.
5. Mattock, A.H. and Hawkins, N.M., "Shear transfer in reinforced concrete – recent research", *PCI Journal*, V. 17, No. 2, Mar.-Apr. 1972, pp. 55-75.
6. Loov, R.E., "Design of precast connections", Paper presented at a seminar organized by Compa International Pte, Ltd. Singapore, 1978, 8 p.
7. Walraven, J., Frénay, J. and Pruijssers, A., "Influence of concrete strength and load history on the shear friction capacity of concrete members", *PCI Journal*, V. 32, No. 1, Jan.-Feb. 1987, pp. 66-84.
8. Randl, N., "Investigations on transfer of forces between old and new concrete at different joint roughness", PhD thesis, University of Innsbruck, 1997, 379 p. (in German)
9. ASTM E 965, "Standard test method for measuring pavement macrotexture depth using a volumetric technique", American Society for Testing Materials, 100 Barr Harbor Dr., West Conshohocken, PA 19428, USA, 2001, 3 p.
10. Santos, P. and Júlio, E., "Development of a laser roughness analyser to predict in situ the bond strength of concrete-to-concrete interfaces", *Magazine of Concrete Research*, V. 60, No. 5, June 2008, pp. 329-337.
11. ICRI (International Concrete Repair Institute), "Selecting and specifying concrete surface preparation for sealers, coatings, and polymer overlays", Technical Guideline No. 03732, Des Plaines, Illinois, USA, 1997, 41 p.
12. Santos, P., Júlio, E. and Silva, V.D., "Correlation between concrete-to-concrete bond strength and the roughness of the substrate surface", *Construction and Building Materials*, V. 21, No. 8, August 2007, pp. 1688-1695.
13. Santos, P.M.D., "Assessment of the shear strength between concrete layers", PhD thesis, Department of Civil Engineering, University of Coimbra, 2009, 338 pp.
14. EN 12615, "Products and systems for the protection and repair of concrete structures – Test methods – Determination of slant shear strength", CEN, 1999.
15. EN 12390-6, "Testing hardened concrete – Part 6: Tensile splitting strength of test specimens", CEN, 2004.
16. EN 12390-3, "Testing hardened concrete – Part 3: Compressive strength of test specimens", CEN, 2003.
17. LNEC E 398, "Concrete – Determination of shrinkage and expansion", LNEC, 2 pp. (in Portuguese)

18. Júlio, E.N.B.S, Branco, F.A., Silva, V.D. and Lourenço, J.F., "Influence of added concrete compressive strength on adhesion to an existing concrete substrate", *Building and Environment*, V. 41, No. 12, December 2006, pp. 1934-1939.
19. Austin, S., Robins P. and Pan, Y., "Shear bond testing of concrete repairs", *Cement and Concrete Research*, V. 29, No. 7, July 1999, pp. 1067-1076.
20. LUSAS - Finite Element System, FEA Ltd, Forge House, 66 High Street, Kingston upon Thames, Surrey, KT1 1HN, United Kingdom